RESEARCH ARTICLE

Figures and figure supplements

A dysmorphic mouse model reveals developmental interactions of chondrocranium and dermatocranium

Susan M Motch Perrine *et al*

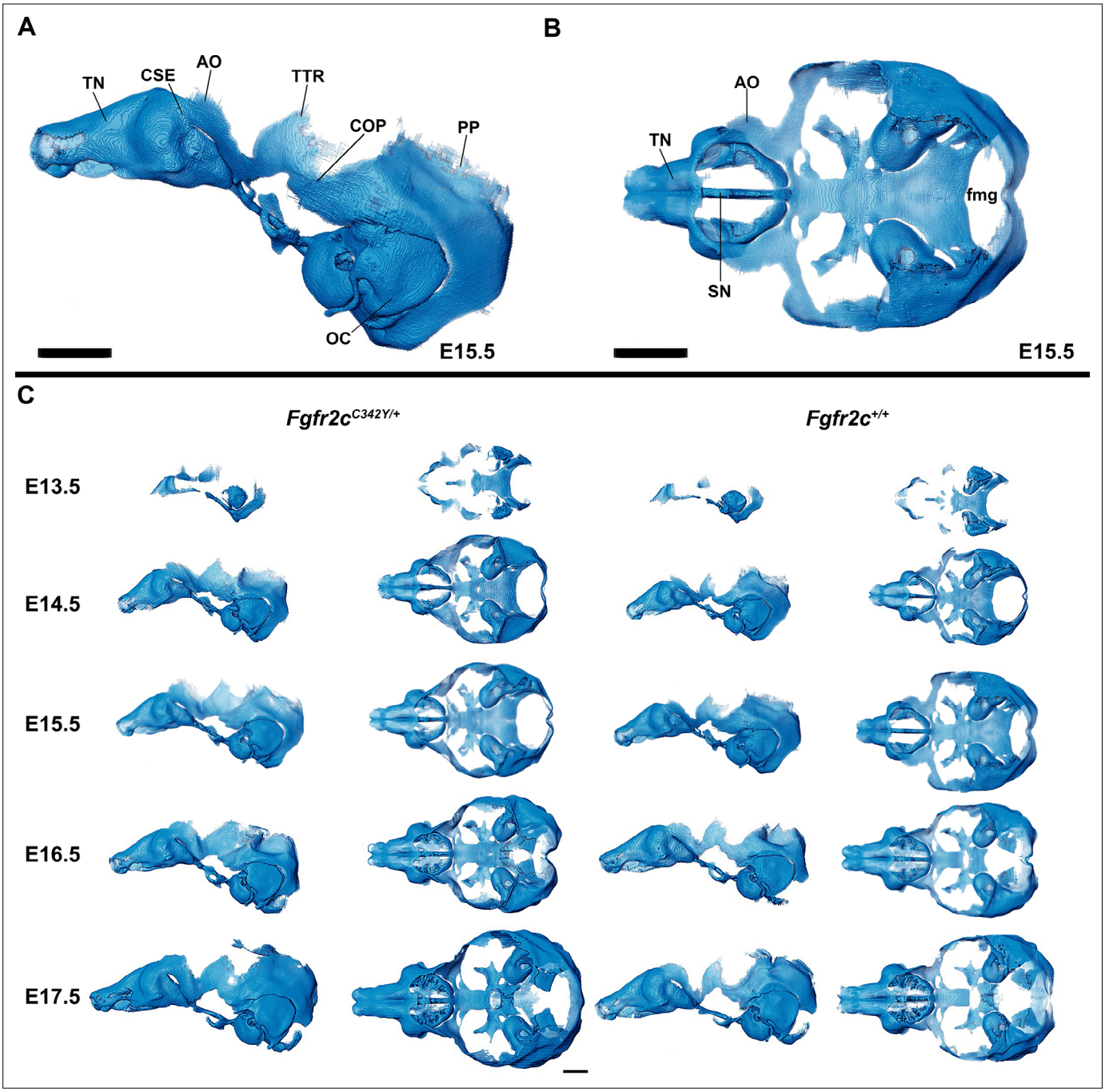

Figure 1. Anatomy of embryonic mouse chondrocranium. (**A, B**) At embryonic day 15.5 (E15.5), the *Fgfr2c*$^{+/+}$ mouse chondrocranium, (**A**) lateral, and (**B**) superior views is complete, consisting of the olfactory region, braincase floor, and lateral walls of the preoccipital and occipital regions. Specific areas of interest include the ala orbitalis (AO), sphenethmoid commissure (CSE), otic capsule (OC), parietal plate (PP), septum nasi (SN), tectum nasi (TN), orbitoparietal commissure (COP), and tectum transversum (TTR) cartilages and the foramen magnum (fmg). (**C**) 3D reconstructions of *Fgfr2c*$^{+/+}$ and *Fgfr2c*$^{C342Y/+}$ chondrocrania from E13.5 to E17.5 in lateral and superior views with nasal capsule to the left. Scale bars = 1 mm. A cartoon of the mouse chondrocranium with more extensive anatomical labeling of cartilages and discussion of their development can be found in ***Kawasaki and Richtsmeier, 2017a*** and ***Kawasaki and Richtsmeier, 2017b***. Interactive viewer of 3D reconstructions can be found at: https://doi.org/10.25550/J-RHCA.

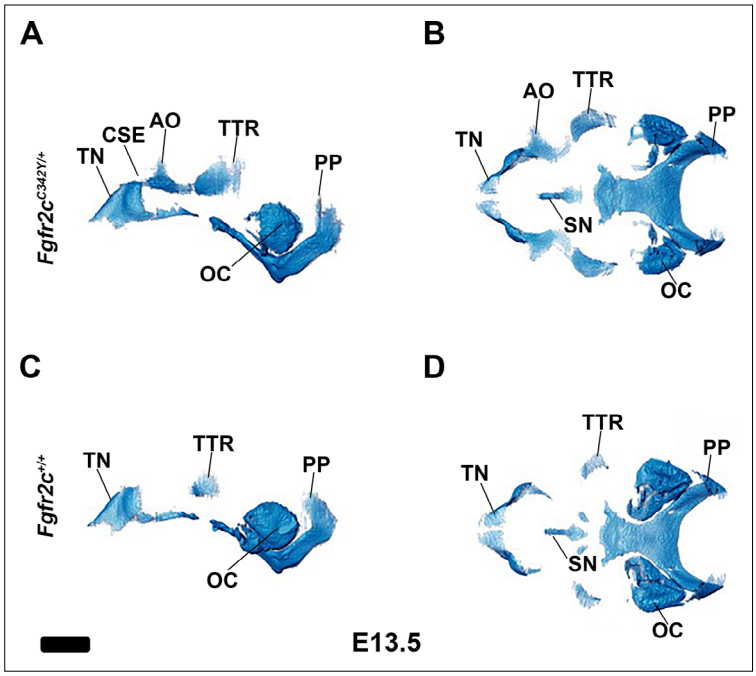

Figure 1—figure supplement 1. Comparison of *Fgfr2c*$^{C342Y/+}$, (**A**) lateral and (**B**) superior views, and *Fgfr2c*$^{+/+}$ (**C**) lateral and (**D**) superior view of mouse embryonic chondrocrania at embryonic day 13.5 (E13.5). Specific areas of interest include the ala orbitalis (AO), sphenethmoid commissure (CSE), otic capsule (OC), parietal plate (PP), septum nasi (SN), tectum nasi (TN), orbitoparietal commissure (COP), and tectum transversum (TTR) cartilages. Note that the CSE and AO are present in the *Fgfr2c*$^{C342Y/+}$ mouse but have not yet developed in the *Fgfr2c*$^{+/+}$ mouse at E13.5. Scale bar = 1 mm.

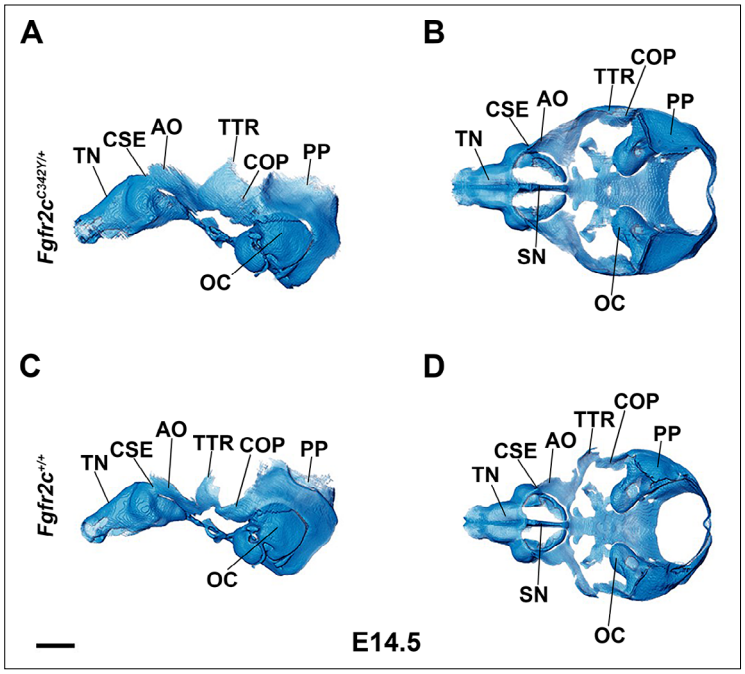

Figure 1—figure supplement 2. Comparison of *Fgfr2c*$^{C342Y/+}$, (**A**) lateral and (**B**) superior views, and *Fgfr2c*$^{+/+}$ (**C**) lateral and (**D**) superior view of mouse embryonic chondrocrania at embryonic day 14.5 (E14.5). Specific areas of interest include the ala orbitalis (AO), sphenethmoid commissure (CSE), otic capsule (OC), parietal plate (PP), septum nasi (SN), tectum nasi (TN), orbitoparietal commissure (COP), and tectum transversum (TTR) cartilages. The AO, TTR, and COP appear more developed in the *Fgfr2c*$^{C342Y/+}$ mouse relative to the *Fgfr2c*$^{+/+}$ mouse with a thick band of cartilage joining AO with TTR. Scale bar = 1 mm.

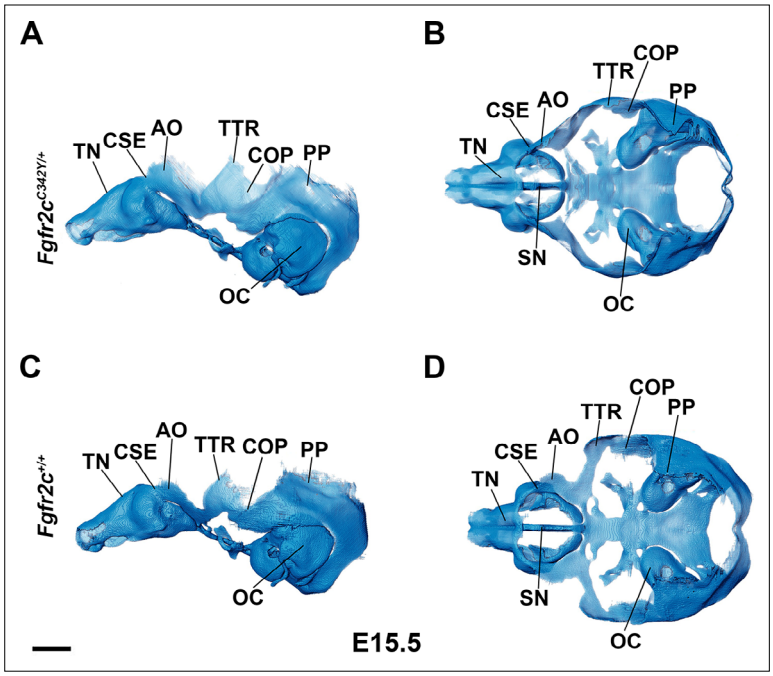

Figure 1—figure supplement 3. Comparison of *Fgfr2c*$^{C342Y/+}$, (**A**) lateral and (**B**) superior views, and *Fgfr2c*$^{+/+}$ (**C**) lateral and (**D**) superior view of mouse embryonic chondrocrania at embryonic day 15.5 (E15.5). Specific areas of interest include the ala orbitalis (AO), sphenethmoid commissure (CSE), otic capsule (OC), parietal plate (PP), septum nasi (SN), tectum nasi (TN), orbitoparietal commissure (COP), and tectum transversum (TTR) cartilages. Note the more robust AO, TTR, and COP in the *Fgfr2c*$^{C342Y/+}$ mouse relative to the *Fgfr2c*$^{+/+}$ mouse with a thick band of cartilage joining AO with TTR. Scale bar = 1 mm.

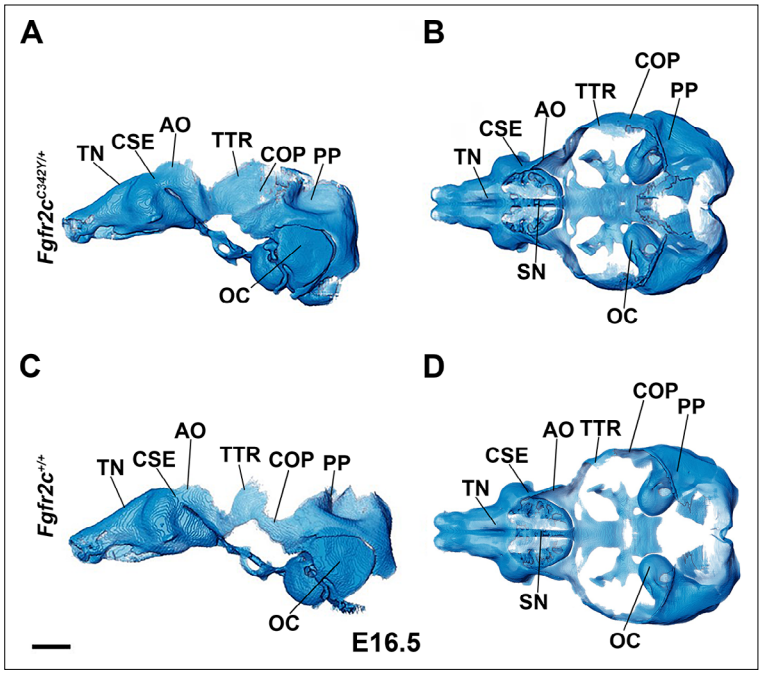

Figure 1—figure supplement 4. Comparison of *Fgfr2c*$^{C342Y/+}$, (**A**) lateral and (**B**) superior views, and *Fgfr2c*$^{+/+}$ (**C**) lateral and (**D**) superior view of mouse embryonic chondrocrania at embryonic day 16.5 (E16.5). Specific areas of interest include the ala orbitalis (AO), sphenethmoid commissure (CSE), otic capsule (OC), parietal plate (PP), septum nasi (SN), tectum nasi (TN), orbitoparietal commissure (COP), and tectum transversum (TTR) cartilages. The chondrocranium of the *Fgfr2c*$^{C342Y/+}$ mouse is more robust with an especially expanded AO, TTR, and COP in the *Fgfr2c*$^{C342Y/+}$ mouse relative to the *Fgfr2c*$^{+/+}$ mouse. Scale bar = 1 mm.

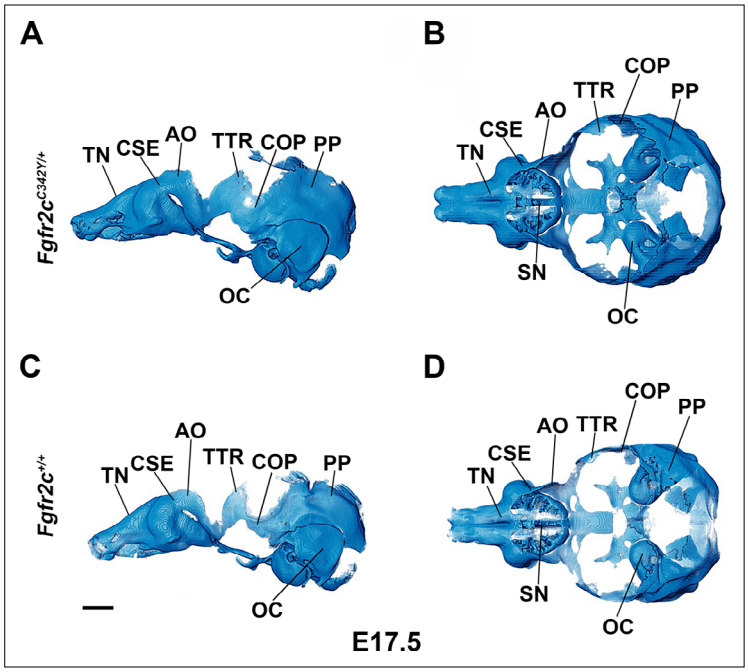

Figure 1—figure supplement 5. Comparison of *Fgfr2c*$^{C342Y/+}$, (**A**) lateral and (**B**) superior views, and *Fgfr2c*$^{+/+}$ (**C**) lateral and (**D**) superior view of mouse embryonic chondrocrania at embryonic day 17.5 (E17.5). The *Fgfr2c*$^{C342Y/+}$ chondrocranium is relatively larger by the naked eye by this age. Specific areas of interest include the ala orbitalis (AO), sphenethmoid commissure (CSE), otic capsule (OC), parietal plate (PP), septum nasi (SN), tectum nasi (TN), orbitoparietal commissure (COP), and tectum transversum (TTR) cartilages. By this time, some cartilages of the lateral wall are disappearing but AO, TTR, and COP remain relatively robust in the *Fgfr2c*$^{C342Y/+}$ mouse relative to the *Fgfr2c*$^{+/+}$ mouse. Scale bar = 1 mm.

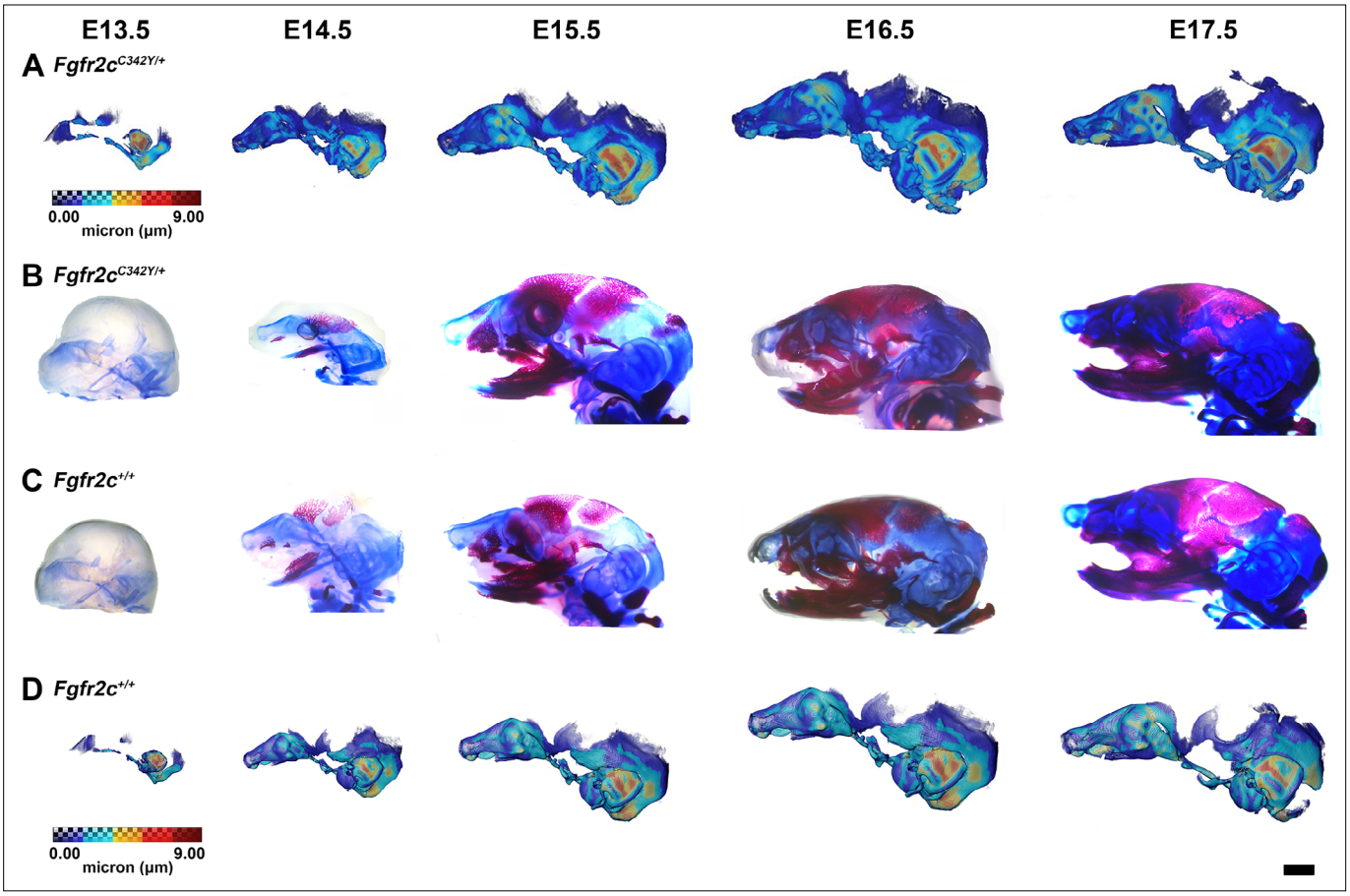

Figure 2. Thickness maps of the chondrocranium of mice segmented from PTA-enhanced micro-computed tomography (microCT) images and similarly aged, cleared, and stained specimens, embryonic day 13.5–17.5 (E13.5–E17.5). (**A, D**) Thickness maps of *Fgfr2c*$^{C342Y/+}$ (**A**) and *Fgfr2c*$^{+/+}$ (**D**) mice segmented from PTA-enhanced microCT images. Colormap indicates cartilage thickness that ranged from just over 0 μm (dark blue) to nearly 9 μm (dark red). (**B, C**) *Fgfr2c*$^{C342Y/+}$ (**B**) and *Fgfr2c*$^{+/+}$ (**C**) specimens that were chemically cleared are stained with Alcian blue indicating proteoglycans in cartilage and alizarin red indicating calcium deposits. Scale bar = 1 mm.

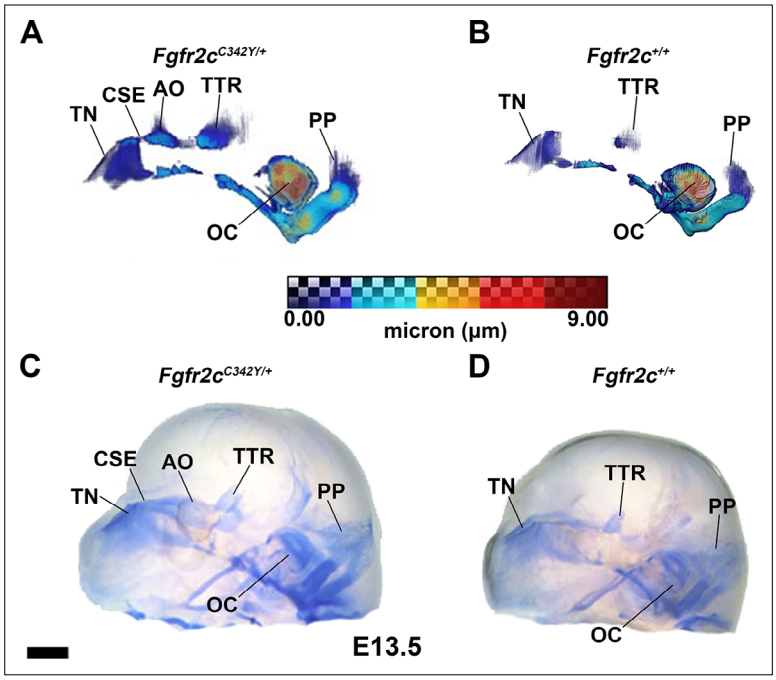

Figure 2—figure supplement 1. Left lateral view of thickness maps of the chodrocrania of mice segmented from phosphotungstic acid (PTA)-enhanced micro-computed tomography (microCT) images of *Fgfr2c*$^{C342Y/+}$ (**A**) and *Fgfr2c*$^{+/+}$ (**B**) mice and cleared and stained *Fgfr2c*$^{C342Y/+}$ (**C**) and *Fgfr2c*$^{+/+}$ (**D**) mice at embryonic day 13.5 (E13.5). Colormap indicates cartilage thickness that ranged from just over 0 μm (dark blue) to nearly 9 μm (dark red). Colormaps of *Fgfr2c*$^{C342Y/+}$ (**A**) and *Fgfr2c*$^{+/+}$ (**B**) chondrocrania in lateral view, segmented from PTA-enhanced microCT images indicate cartilage thicknesses that ranged from just over 0 μm (dark blue) to nearly 9 μm (dark red). The *Fgfr2c*$^{C342Y/+}$ (**C**) and *Fgfr2c*$^{+/+}$ (**D**) specimens that were chemically cleared and stained with Alcian blue indicating proteoglycans in cartilage and alizarin red indicating calcium containing osteocytes. Cartilaginous structures of interest include the ala orbitalis (AO), sphenethmoid commissure (CSE), otic capsule (OC), parietal plate (PP), septum nasi (SN), tectum nasi (TN), orbitoparietal commissure (COP), and tectum transversum (TTR). Note that the CSE and AO are present in the *Fgfr2c*$^{C342Y/+}$ embryo but have not yet developed in the *Fgfr2c*$^{+/+}$ embryo at E13.5. No osteocyte containing bone is shown in either genotype at this age. Scale bar = 1 mm.

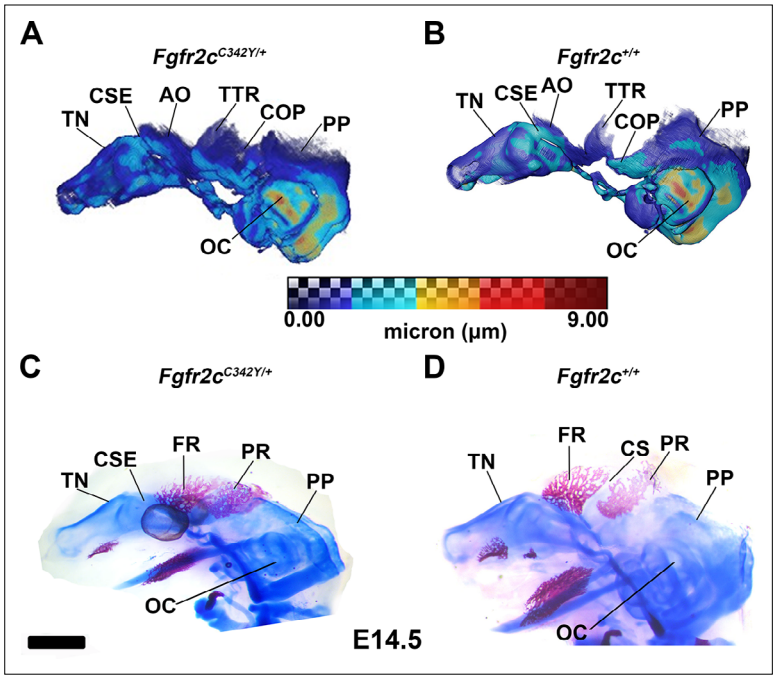

Figure 2—figure supplement 2. Left lateral view of thickness maps of the chodrocrania of mice segmented from phosphotungstic acid (PTA)-enhanced micro-computed tomography (microCT) images of *Fgfr2c*$^{C342Y/+}$ (**A**) and *Fgfr2c*$^{+/+}$ (**B**) mice and cleared and stained *Fgfr2c*$^{C342Y/+}$ (**C**) and *Fgfr2c*$^{+/+}$ (**D**) mice at embryonic day 14.5 (E14.5). Colormap indicates cartilage thickness that ranged from just over 0 μm (dark blue) to nearly 9 μm (dark red). Colormaps of *Fgfr2c*$^{C342Y/+}$ (**A**) and *Fgfr2c*$^{+/+}$ (**B**) chondrocrania in lateral view, segmented from PTA-enhanced microCT images indicate cartilage thicknesses that ranged from just over 0 μm (dark blue) to nearly 9 μm (dark red). Comparable areas of cartilage development identified in *Fgfr2c*$^{C342Y/+}$ (**C**) and *Fgfr2c*$^{+/+}$ (**D**) specimens that were chemically cleared and stained with Alcian blue indicating proteoglycans in cartilage. Developing bone is shown using alizarin red staining indicating calcium containing osteocytes. Specific cartilages of interest include the ala orbitalis (AO), sphenethmoid commissure (CSE), otic capsule (OC), parietal plate (PP), septum nasi (SN), tectum nasi (TN), orbitoparietal commissure (COP), and tectum transversum (TTR) cartilages. Note the more developed AO, TTR, and COP in the *Fgfr2c*$^{C342Y/+}$ mouse relative to the *Fgfr2c*$^{+/+}$ mouse. The frontal (FR) and parietal (PR) bones are separated by a presumptive coronal suture (CS) in the *Fgfr2c*$^{+/+}$ specimen (**D**), but there is no comparable separation of the frontal and parietal bones in the *Fgfr2c*$^{C342Y/+}$ mouse (**C**) suggesting a lack of suture formation. Scale bar = 1 mm.

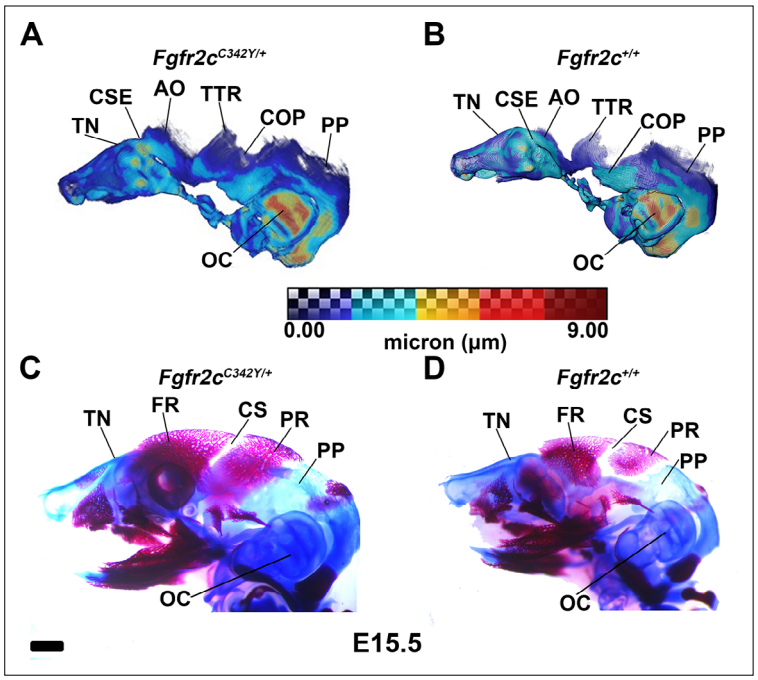

Figure 2—figure supplement 3. Left lateral view of thickness maps of the chodrocrania of mice segmented from phosphotungstic acid (PTA)-enhanced micro-computed tomography (microCT) images of *Fgfr2c*$^{C342Y/+}$ (**A**) and *Fgfr2c*$^{+/+}$ (**B**) mice and cleared and stained *Fgfr2c*$^{C342Y/+}$ (**C**) and *Fgfr2c*$^{+/+}$ (**D**) mice at embryonic day 15.5 (E15.5). Colormap indicates cartilage thickness that ranged from just over 0 μm (dark blue) to nearly 9 μm (dark red). Colormaps of *Fgfr2c*$^{C342Y/+}$ (**A**) and *Fgfr2c*$^{+/+}$ (**B**) chondrocrania in lateral view, segmented from PTA-enhanced microCT images indicate cartilage thicknesses that ranged from just over 0 μm (dark blue) to nearly 9 μm (dark red). Thickness maps show larger, thicker AO, TTR, and COP in the *Fgfr2c*$^{C342Y/+}$ mouse relative to the *Fgfr2c*$^{+/+}$ mouse. The *Fgfr2c*$^{C342Y/+}$ (**C**) and *Fgfr2c*$^{+/+}$ (**D**) specimens that were chemically cleared and stained with Alcian blue indicating proteoglycans in cartilage and alizarin red indicating calcium containing osteocytes indicate a large degree of dermal bone formation between E14.5 and E15.5. Most of the anterior cartilages (ala orbitalis [AO], sphenethmoid commissure [CSE], septum nasi [SN], tectum nasi [TN], orbitoparietal commissure [COP], and tectum transversum [TTR] cartilages) are covered by dermal bone. The otic capsule (OC) and parietal plate (PP) remain visible In these specimens, the frontal (FR) and parietal (PR) bones are separated by the coronal suture (CS) in both genotypes (**C, D**). Scale bar = 1 mm.

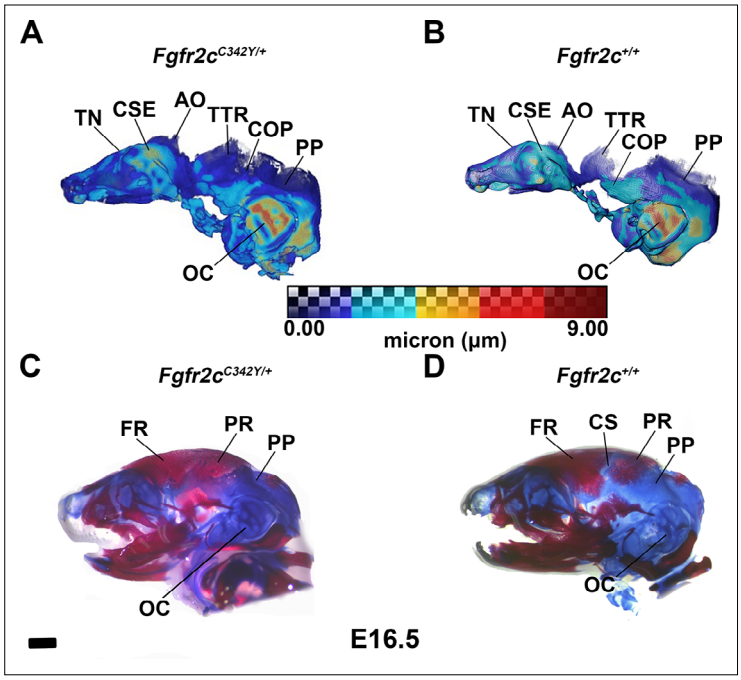

Figure 2—figure supplement 4. Left lateral view of thickness maps of the chodrocrania of mice segmented from phosphotungstic acid (PTA)-enhanced micro-computed tomography (microCT) images of *Fgfr2c*$^{C342Y/+}$ (**A**) and *Fgfr2c*$^{+/+}$ (**B**) mice and cleared and stained *Fgfr2c*$^{C342Y/+}$ (**C**) and *Fgfr2c*$^{+/+}$ (**D**) mice at embryonic day 16.5 (E16.5). Colormap indicates cartilage thickness that ranged from just over 0 μm (dark blue) to nearly 9 μm (dark red). Colormaps of *Fgfr2c*$^{C342Y/+}$ (**A**) and *Fgfr2c*$^{+/+}$ (**B**) chondrocrania in lateral view, segmented from PTA-enhanced microCT images indicate cartilage thicknesses that ranged from just over 0 μm (dark blue) to nearly 9 μm (dark red). The entire chondrocranium of *Fgfr2c*$^{C342Y/+}$ embryos is relatively robust with the tectum nasi (TN), ala orbitalis (AO), and tectum transversum (TTR) showing obvious thickness differences between genotypes. *Fgfr2c*$^{C342Y/+}$ (**C**) and *Fgfr2c*$^{+/+}$ (**D**) specimens that were chemically cleared and stained with Alcian blue indicating proteoglycans in cartilage and alizarin red indicating calcium containing osteocytes. The frontal (FR) and parietal (PR) bones are separated by the coronal suture (CS) in the *Fgfr2c*$^{+/+}$ specimen (**D**), but the suture is obliterated in the *Fgfr2c*$^{C342Y/+}$ mouse (**C**). The interparietal bone has formed in both geneotypes. Scale bar = 1 mm.

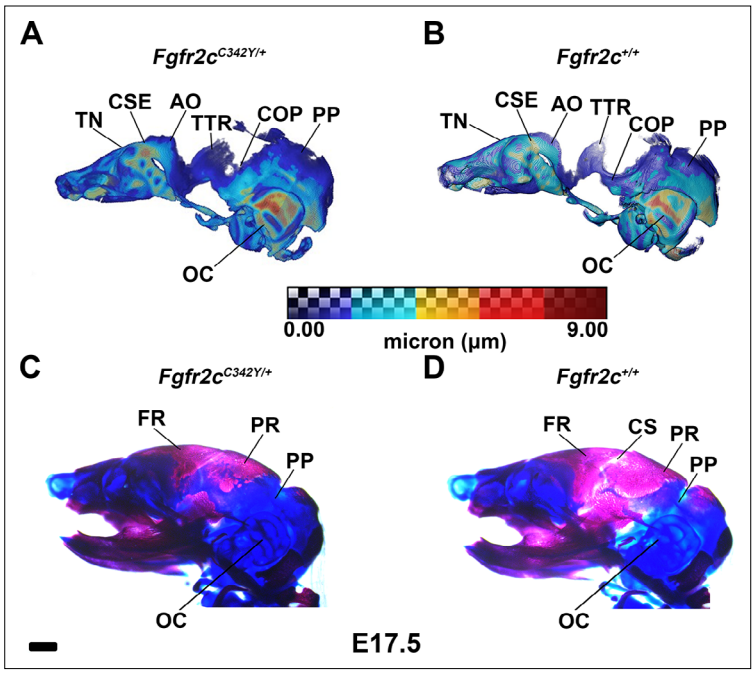

Figure 2—figure supplement 5. Left lateral view of thickness maps of the chodrocrania of mice segmented from phosphotungstic acid (PTA)-enhanced micro-computed tomography (microCT) images of *Fgfr2c*$^{C342Y/+}$ (**A**) and *Fgfr2c*$^{+/+}$ (**B**) mice and cleared and stained *Fgfr2c*$^{C342Y/+}$ (**C**) and *Fgfr2c*$^{+/+}$ (**D**) mice at embryonic day 17.5 (E17.5). Colormap indicates cartilage thickness that ranged from just over 0 μm (dark blue) to nearly 9 μm (dark red). Colormaps of *Fgfr2c*$^{C342Y/+}$ (**A**) and *Fgfr2c*$^{+/+}$ (**B**) chondrocrania in lateral view, segmented from PTA-enhanced microCT images indicate cartilage thicknesses that ranged from just over 0 μm (dark blue) to nearly 9 μm (dark red). Though the chondrocranium is beginning to dissolve in both genotypes, this process appears to be more advanced in *Fgfr2c*$^{C342Y/+}$ embryos, with the ala orbitalis (AO) and tectum transversum (TTR) becoming noticeably thin. *Fgfr2c*$^{C342Y/+}$ (**C**) and *Fgfr2c*$^{+/+}$ (**D**) specimens that were chemically cleared and stained with Alcian blue indicating proteoglycans in cartilage and alizarin red indicating calcium containing osteocytes. At this age, it is difficult to distinguish separate cartilages and bones in cleared and stained specimens. However, frontal (FR) and parietal (PR) bones are separated by the coronal suture (CS) in the *Fgfr2c*$^{+/+}$ specimen (**D**), and there is no suture in the *Fgfr2c*$^{C342Y/+}$ embryo (**C**). Scale bar = 1 mm.

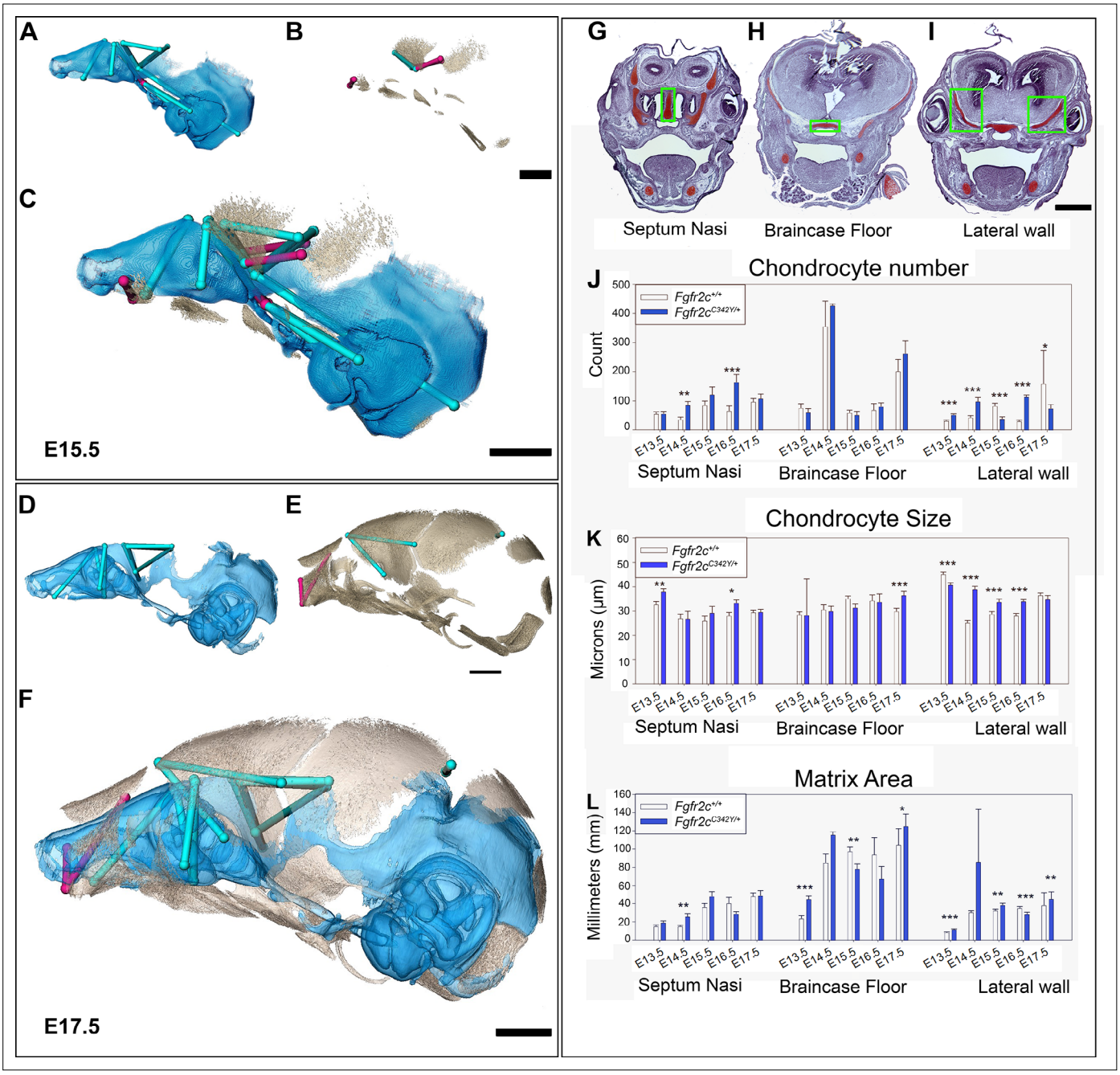

Figure 3. Euclidean distance matrix analysisDistance Matrix Analysis of the chondrocranium and bony skull, and histomorphology of the chondrocranium. Linear distances of the chondrocranium (**A, D**), bony skull (**B, E**), and the two superimposed (**C, F**) that are statistically significantly different between genotypes by confidence interval testing (α=0.10). Blue lines indicate linear distances that are significantly larger in *Fgfr2c*$^{C342Y/+}$ mice; fuchsia lines are significantly reduced in *Fgfr2c*$^{C342Y/+}$ mice. (**A–F**) Significant differences between chondrocranium and bony skulls of *Fgfr2c*$^{C342Y/+}$ and *Fgfr2c*$^{+/+}$mice. A limited landmark set common to the chondrocranium and bony skull of embryonic day 15.5 (E15.5) (**A–C**) and E17.5 (**D–F**) embryos was used for analyses and indicated that the lateral wall and olfactory regions are most different between *Fgfr2c*$^{C342Y/+}$ and *Fgfr2c*$^{+/+}$ mice at these ages. (**G–L**) Histomorphology of the chondrocranium. Histological sections of the E15.5 chondrocranium highlighting the septum nasi (**G**), braincase floor (**H**), and lateral walls (**I**) in green boxes. These areas were assessed at E13.5, E14.5, E15.5, E16.5, and E17.5 for chondrocyte number (**J**), chondrocyte size (**K**), and area of cartilaginous matrix (**L**) in *Fgfr2c*$^{C342Y/+}$ and *Fgfr2c*$^{+/+}$ mice. In agreement with the larger chondrocrania of *Fgfr2c*$^{C342Y/+}$ mice, there are localized regions that reveal increases in chondrocyte number, size, and/or contribution of matrix at each timepoint. Note the trend of increasing numbers of chondrocytes over time as expected in a growing chondrocranium. For histological analysis data are displayed as mean +/- standard error of at least three quantified images per individual (n) per region per age compared between genotypes using non-parametric Mann-Whitney U tests; *p≤0.05, **p≤0.01, ***p≤0.001. n (*Fgfr2c*$^{+/+}$/*Fgfr2c*$^{C342Y/+}$) = 4/4(E13.5), 7/7 (E14.5), 6/6 (E15.5), 6/5 (E16.5), 4/5 (E17.5). Scalebars = 1mm.

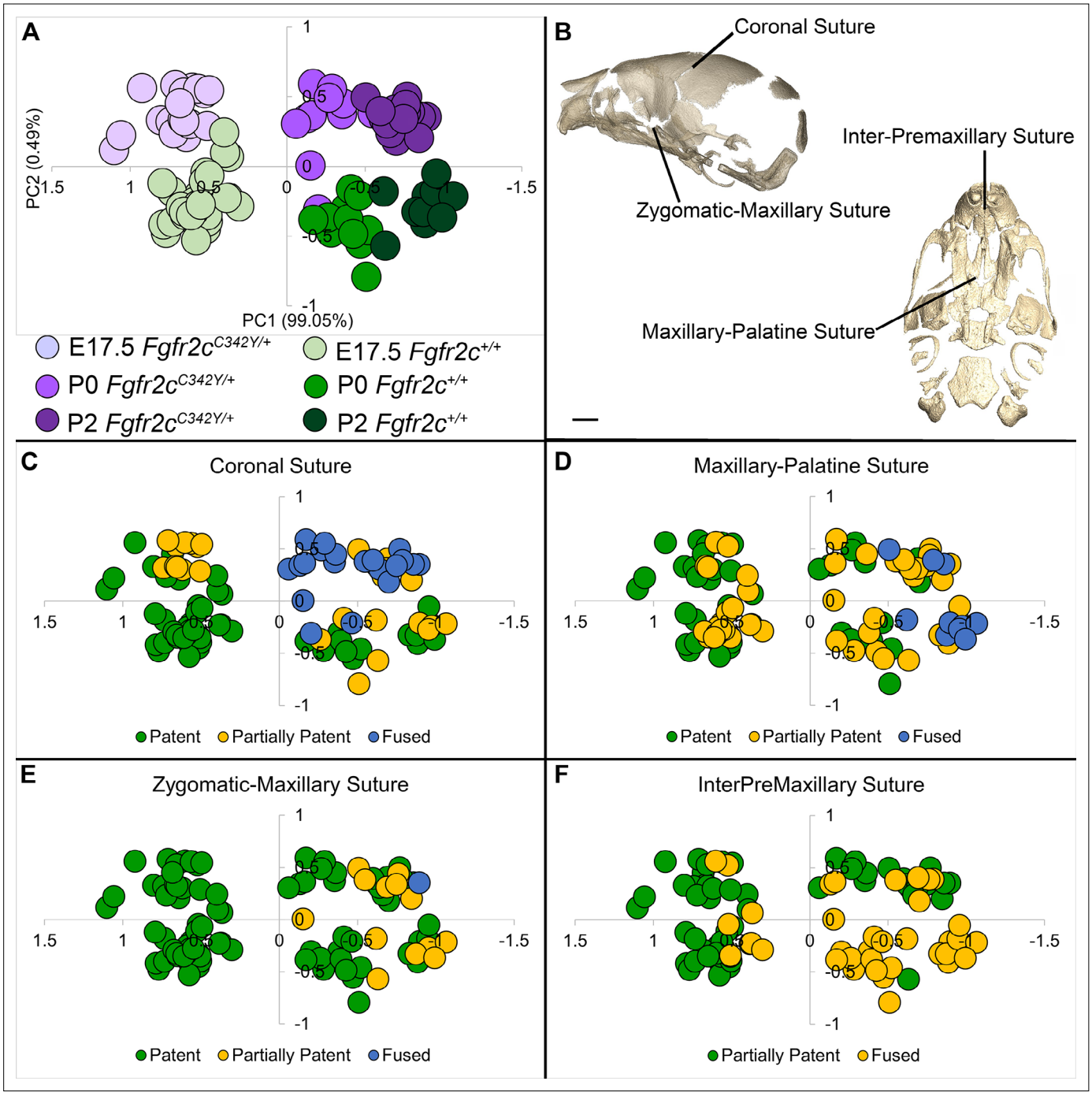

Figure 4. Relationship of suture patency patterns and craniofacial shape as estimated by principal components analysis (PCA). (**A**) PCA of skull linear distance data estimated from 3D landmark locations collected from micro-computed tomography (microCT) images of mice at E17.5, postnatal day 0 (P0), and P2 shows distribution of all individuals along principal component 1 (PC1) and PC2. (**B**) Suture patency was scored for sutures as visualized on left lateral and inferior views of a microCT 3D reconstruction of a *Fgfr2c*$^{+/+}$ P0 skull. (**C–F**) Distribution of individuals along PC1 and PC2 as shown in (**A**) coded for patency of the coronal suture (**C**), the maxillary-palatine suture (**D**), the zygomatic-maxillary suture (**E**), and the inter-premaxillary suture (**F**). Scale bar = 1 mm.

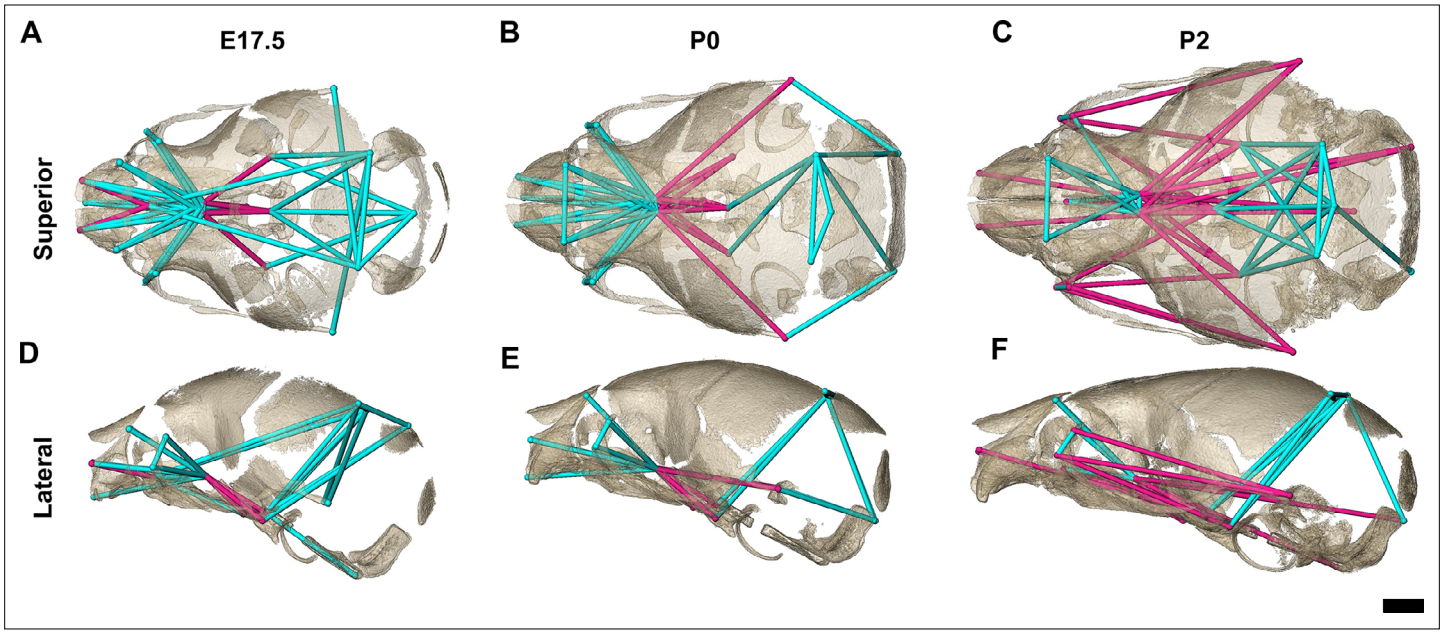

Figure 5. Euclidean distance matrix analysis of the bony skull during late prenatal and early postnatal stages. Increased mineralization allowed a larger set of landmarks to be used for statistical comparison of skull shape between genotypes at embryonic day 17.5 (E17.5), postnatal day 0 (P0), and P2 (as compared to ***Figure 3***). Superior (**A–C**) and lateral (**D–F**) views of linear distances of the bony skull that are statistically significantly different between genotypes by confidence interval testing (α=0.10) shown on the dermatocranium of a *Fgfr2c*$^{+/+}$ mouse at E17.5 (**A, D**), P0 (**B, E**), and P2 (**C, F**). Blue lines indicate linear distances that are significantly larger in *Fgfr2c*$^{C342Y/+}$ mice; fuchsia lines indicate linear distances that are significantly reduced in *Fgfr2c*$^{C342Y/+}$ mice. Quantitative patterns reveal a reversal in relative size postnatally, with the *Fgfr2c*$^{C342Y/+}$ skull becoming generally smaller than skulls of *Fgfr2c*$^{+/+}$ littermates. Scalebar = 1 mm.

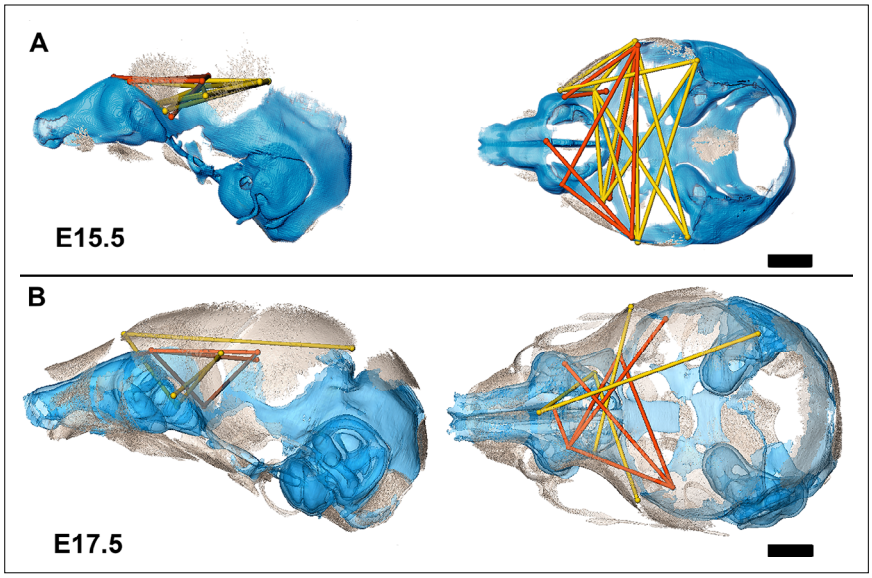

Figure 6. Summary of statistically significant differences in morphological integration of dermatocranium and chondrocranium between genotypes with two videos. (**A**) Linear distance pairs from the dermatocranium (yellow) and chondrocranium (orange) whose association is statistically stronger (α=0.10) in *Fgfr2c*$^{C342Y/+}$ mice relative to *Fgfr2c*$^{+/+}$ mice at embryonic day 15.5 (E15.5) and (**B**) at E17.5. Left lateral (at left) and superior (at right) views shown. Scalebars = 1 mm.